Molecular Oncology

CrossMark

Molecular correlates of platinum response in human high-grade serous ovarian cancer patient-derived xenografts

Monique D. Topp[a,b], Lynne Hartley[a], Michele Cook[a], Valerie Heong[a,c,d], Emma Boehm[a], Lauren McShane[a], Jan Pyman[c], Orla McNally[c], Sumitra Ananda[c], Marisol Harrell[e], Dariush Etemadmoghadam[f,g,h], Laura Galletta[f], Kathryn Alsop[f], Gillian Mitchell[f], Stephen B. Fox[f,h], Jeffrey B. Kerr[b], Karla J. Hutt[b,i], Scott H. Kaufmann[j], Australian Ovarian Cancer Study[f,k,l,m], Elizabeth M. Swisher[e], David D. Bowtell[f,g,n], Matthew J. Wakefield[a,d,o,1], Clare L. Scott[a,c,d,*,1]

[a]The Walter and Eliza Hall Institute of Medical Research, Parkville, Victoria 3052, Australia
[b]Department of Medicine and Health Sciences, Monash University, Clayton, Victoria 3168, Australia
[c]Royal Women's Hospital, Parkville, Victoria 3052, Australia
[d]Department of Medical Biology, University of Melbourne, Parkville, Victoria 3052, Australia
[e]University of Washington, Seattle, WA, USA
[f]Peter MacCallum Cancer Centre, East Melbourne, Victoria 8006, Australia
[g]Sir Peter MacCallum Department of Oncology, University of Melbourne, Melbourne, Victoria 3010, Australia
[h]Department of Pathology, University of Melbourne, Melbourne, Victoria 3010, Australia
[i]Prince Henry's Institute of Medical Research, Clayton, Victoria 3168, Australia
[j]Mayo Clinic Cancer Centre, Rochester, MN, USA
[k]Westmead Institute for Cancer Research, University of Sydney at Westmead Millennium Institute, Westmead Hospital, NSW, Australia
[l]Department of Gynaecological Oncology, Westmead Hospital, NSW, Australia
[m]Queensland Institute of Medical Research, Brisbane, QLD, Australia
[n]Department of Biochemistry and Molecular Biology, University of Melbourne, Melbourne, Victoria 8006, Australia
[o]Department of Genetics, University of Melbourne, Melbourne, Victoria 8006, Australia

ARTICLE INFO

ABSTRACT

Introduction: Improvement in the ability to target underlying drivers and vulnerabilities of high-grade serous ovarian cancer (HG-SOC) requires the development of molecularly annotated pre-clinical models reflective of clinical responses.

Methods: We generated patient-derived xenografts (PDXs) from consecutive, chemotherapy-naïve, human HG-SOC by transplanting fresh human HG-SOC fragments into subcutaneous and intra-ovarian bursal sites of NOD/SCID IL2Rγ[null] recipient mice, completed molecular annotation and assessed platinum sensitivity.

Results: The success rate of xenografting was 83%. Of ten HG-SOC PDXs, all contained mutations in *TP53*, two were mutated for *BRCA1*, three for *BRCA2*, and in two, *BRCA1* was methylated.

Platinum
Xenograft
DNA repair
BRCA1
BRCA2

In vivo cisplatin response, determined as platinum sensitive (progression-free interval $\geq$100 d, $n = 4$), resistant (progression-free interval <100 d, $n = 3$) or refractory ($n = 3$), was largely consistent with patient outcome. Three of four platinum sensitive HG-SOC PDXs contained DNA repair gene mutations, and the fourth was methylated for *BRCA1*. In contrast, all three platinum refractory PDXs overexpressed dominant oncogenes (*CCNE1*, *LIN28B* and/or *BCL2*).
Conclusions: Because PDX platinum response reflected clinical outcome, these annotated PDXs will provide a unique model system for preclinical testing of novel therapies for HG-SOC.

1. Introduction

Epithelial ovarian cancer (OC) remains the most lethal of gynecological malignancies, with over 70% of cases resulting in mortality. Improvement in our ability to target the underlying drivers and vulnerabilities of sub-groups of OC requires the development of molecularly annotated pre-clinical models that reflect clinical responses and can be utilized to test novel therapies (Bookman, 2011). Recently, however, five of the most frequently utilized ovarian cancer cell lines, which are generally employed to model the most common and aggressive OC subtype, high-grade serous OC (HG-SOC), were shown to lack the common genetic features of HG-SOC (Domcke et al., 2013). These observations highlight the urgent need to develop and characterize new HG-SOC models that more accurately reflect the biology of this neoplasm.

HG-SOC has been characterized as a disease of genomic instability, with relatively few recurrent somatic mutations or dominantly acting oncogenes (TCGA (2011)). At present, standard-of-care therapy for women with advanced OC includes cytoreductive surgery and platinum/taxane-based chemotherapy. Factors underlying response and resistance to platinum-based therapy in HG-SOC remain incompletely understood. Progress in the development of novel therapeutics in OC has been hampered by lack of biomarkers that permit appropriate targeting of new agents. Access to serial biopsies of human OC, before and after treatment, is recommended as a central component of clinical trial design (Vaughan et al., 2011) but has been slow to occur.

At present, response to platinum chemotherapy is the strongest predictor of survival for women with HG-SOC (Bookman et al., 2009). Patients with platinum-sensitive OC, defined as clinical response for at least six months following cessation of primary platinum therapy, have a better overall survival than patients with either platinum-resistant disease (relapse <6 months following cessation of primary platinum therapy) or platinum-refractory disease (progressive disease while on primary platinum therapy). These variations in response appear to reflect, at least in part, differences in integrity of the homologous recombination (HR) DNA repair pathway, which contains mutations in up to 50% of HG-SOCs (2011). In particular, HR-compromising *BRCA1* or *BRCA2* mutations occur in 18—21% of HG-SOC (TCGA, 2011; Walsh et al., 2011) and are associated with improved response to DNA damaging chemotherapy (Alsop et al., 2012; Kaye et al., 2012; TCGA, 2011) as well as PARP inhibitors (Audeh et al., 2010; Ledermann et al., 2012). Conversely, secondary somatic

mutations or "reversions" that restore *BRCA1/2* (Edwards et al., 2008; Sakai et al., 2008) in OC from women with germline *BRCA1/2* mutations predict acquired resistance to platinum or PARP inhibitor therapy (Barber et al., 2013; Norquist et al., 2011). Despite the clinical importance of *BRCA1/2* mutations, established human OC cell lines contain *BRCA1* and *BRCA2* mutations only rarely (Domcke et al., 2013; Stordal et al., 2013), further highlighting the limitations of current pre-clinical OC models for therapeutic studies.

Additional changes with the potential to effect platinum sensitivity have also been observed in OC. *CCNE1* has been shown to be associated with resistance to platinum drugs based on an empiric screen of platinum resistant HG-SOC (Etemadmoghadam et al., 2010) and was the most common amplification identified by TCGA (TCGA (2011)). The MYCN pathway was the oncogenic pathway associated with the proliferative subgroup of HG-SOC, identified by hierarchical clustering (Helland et al., 2011). Overexpression or amplification of pro-survival oncogenic members of the *BCL2* family has been observed (Beroukhim et al., 2010) and has been associated with diminished efficiency of targeted therapeutics as well as classical cytotoxics (Cragg et al., 2009).

Previous reports of molecularly annotated PDXs derived from unmanipulated HG-SOC for pre-clinical evaluation are extremely limited. Most OC animal models have been generated from murine ovarian surface epithelial cell lines (ID8 cells) (Roby et al., 2000) or by xenografting established human HG-SOC cell lines, which are often of poorly-defined origin and have been in culture for many years (Domcke et al., 2013). In contrast, even though PDXs from primary HG-SOC retain pathological and immunohistochemical features of the primary tumor (Lee et al., 2005) and have been used to study tumor-initiating cell frequency (Stewart et al., 2011), the response of these PDXs to conventional or targeted therapeutics has only been described for a handful of individual PDX models (e.g., 1—2 independent HG-SOC PDX per report (Faratian et al., 2011; Kortmann et al., 2011; Press et al., 2008; Sims et al., 2012)) in the context of molecular annotation or patient outcome data.

To determine i) whether the major genetic changes observed in HG-SOCs are retained in PDXs, ii) compare the responses of PDXs and the clinical tumors in the same patients, and iii) develop an *in vivo* model for preclinical studies that more closely represents the biology of HG-SOC, we transplanted consecutive chemotherapy-naive fresh human HG-SOC fragments without prior *in vitro* culture and drove platinum resistance with first- and subsequent-line cisplatin

regimens. This cohort of HG-SOC PDXs, annotated according to the major clinical prognostic features of *in vivo* cisplatin response and DNA repair gene status, represents a novel resource for testing future therapeutic strategies.

2.   Methods

2.1.   Clinical samples

Samples were collected from chemotherapy naïve patients enrolled in the Australian Ovarian Cancer Study who underwent surgery at the Royal Women's Hospital. The Australian Ovarian Cancer Study was approved by the Human Research Ethics Committees at the Peter MacCallum Cancer Centre, Queensland Institute of Medical Research, University of Melbourne and all participating hospitals. Additional approval was obtained from the Human Research Ethics Committees at the Royal Women's Hospital and the Walter and Eliza Hall Institute. Clinical follow-up of patient outcome was obtained via the CONTRO-engined gemma database, Royal Women's Hospital. Due to concerns regarding maintaining patient deidentification in this consecutive, single institution series, some clinical details have not been presented.

2.2.   Immunohistochemistry

Automated staining was performed with a Ventana BenchMark Ultra (Roche Diagnostics, USA). The following clones from Ventana were used: for WT1 (6F-H2); PAX8 (MRQ-50), ER (SP1); PR (1E2); Ki67 (30-9); p53 (DO-7) and Anti-Pan Keratin (AE1/AE3/PCK26). All first generation (T1) xenografts (human tumor tissue transplanted into a mouse, arising as a xenograft), were screened with immunohistochemistry (IHC) for human CD45 (RP2.18, Ventana), in order to exclude occasional donor-derived hematologic malignancy (transplantable). Sections stained for Bcl-2 and Cyclin E were scored by two investigators blinded as to HG-SOC/PDX number. Consecutive high-powered fields and 200 consecutive tumor cells were assessed for staining. Percent of strong (+++), moderate (++), low (+) and absent staining was documented ((+++% $\times$ 3) + (++% $\times$ 2) + (+% $\times$ 1) + (0% $\times$ 0), out of a possible total score of 300).

2.3.   qRT-PCR

Total RNA was extracted from snap frozen tumor material and RNA later samples and converted to cDNA and analysed in qPCR 15 uL reaction volume using primers for *MYCN*, *LIN28B*, *LIN28A*, *HMGA2*, *CCNE1*, *HPRT* and, as an endogenous normalization control, *ACTB* (*β-actin*) with SYBR-green reagent (Qiagen) and assessed on an ABI-PRISM 7900 thermal cycler (both from Applied Biosystems). Data analyses were performed by the comparative threshold cycle method (Narita et al., 2003). For each baseline HG-SOC, one aliquot of RNA was generated and used in 3–7 independent experiments. The positive control for the MYCN pathway was the CH1 cell line, which has increased expression of MYCN, although not copy number gain (Helland et al., 2011). The positive control for *CCNE1* overexpression was the OVCAR3 cell line, which has high-level

amplification of *CCNE1* (log 2 CN ratio >2 by qRT-PCR and SNP microarray) (Etemadmoghadam et al., 2010).

2.4.   Generation of patient-derived xenografts (PDX)

Immuno-compromised nonobese diabetic-severe combined immunodeficient, interleukin -2 receptor-γ-null (NOD-SCID-IL-2rγ) mice (4–8 wk old; WEHI animal breeding facility) were used for animal studies with approval from the Melbourne Health Animal Ethics Committee and the WEHI Animal Ethics Committee. Under anaesthesia, a fragment of fresh tumor was placed subcutaneously (1–3 mm^3) or via the intra-ovarian bursal (<1 mm^3) approach. Tumor growth was monitored by measuring 2 perpendicular axes using calipers once weekly and tumor volume calculated as $\pi/6 \times$ [larger diameter $\times$ smaller diameter^2]). The mouse was sacrificed once the tumor volume reached 0.7 cm^3. The tumor was harvested and prepared as above for analysis as well as being transplanted into new recipient mice to generate serial propagation. Tumor material was minced and viably frozen in 10% DMSO in liquid nitrogen ensuring continuation of the resource.

2.5.   In vivo cisplatin treatments

Recipient mice bearing tumors ~0.2 cm^3 in size (0.18–0.3 cm^3) were randomly assigned to weekly treatment with vehicle or cisplatin (4 mg/kg) on days 1, 8 and 18. This regimen was chosen based on dose titration/timing studies in tumor-bearing NOD-SCID-IL-2rγ mice. Tumor growth was monitored as above 2–3 $\times$ weekly and tumor volume calculated. The mouse was sacrificed once the tumor volume reached 0.7 cm^3. The tumor was harvested and prepared as above for analysis as well as being transplanted into new recipient mice for second- and third-line cisplatin therapy. Mice were bled at cull for hematologic analysis if unwell or for storage of plasma at $-80\,^\circ$C. For a subset of mice, when tumors reached 0.5 cm^3, mice were retreated with the same treatment regimen and/or were euthanized when tumors reached 0.7 cm^3.

Time to Progressive disease (PD) was defined as the time (in days) from beginning of treatment to an increase in average tumor volume (for that treatment group) of >20% from the nadir (taken as the smallest average tumor volume recorded since treatment started or 0.2 cm^3 if nadir was <0.2 cm^3 as lesions smaller than this are difficult to measure with accuracy) (Supplementary Table S6).

Time to Harvest (TTH) was defined as the time (in days) from the beginning of treatment to day of harvest at 0.7 cm^3 and the median TTH was calculated and plotted using Kaplan–Meier curves (Prism version 5) (Supplementary Table S6).

Time to re-treatment for an individual mouse was defined as the time (in days) from the last day of treatment to first day of re-treatment (treatment free interval) of that mouse which occurred when tumor volume reached 0.5 cm^3. This was then compared with time from last day of re-treatment to day when tumor volume for that mouse reached 0.5 cm^3 (Supplementary Table S7).

One hundred days was chosen as a conservative measure to differentiate between cisplatin sensitivity versus resistance

for PDX, as PD usually occurred around 50 d or earlier, or in contrast, sustained remission was also observed (>200 d). The six-month timeline used to determine platinum sensitivity in the clinic was not reasonable, as that represents one quarter of a mouse's lifetime, and around one third of the life-time of an immuno-compromised mouse. T2 PDX derived from different T1 PDX mice (bearing the same PDX, e.g., #11) had similar cisplatin response.

2.6. Sequencing of HG-SOC tumor material

BROCA sequencing was performed as previously described with some modifications (Walsh et al., 2011). DNA was sonicated to a peak of 200 bp on a Covaris E series instrument (Covaris, Woburn, MA). Paired end libraries were prepared in 96 well plate format using the SureSelectXT enrichment system on a Bravo liquid-handling instrument (Agilent, Santa Clara CA). Individual paired end libraries (500 ng) were hybridized to a 1.5 Mb custom design of cRNA biotinylated oligonucleotides targeting 42 genomic regions (Supplementary Table S3). Following capture, each library was PCR amplified with primers containing a unique 6bp index and quantified by High Sensitivity chip (Agilent, Santa Clara CA). Equimolar concentrations of 96 libraries were pooled to a final concentration of 11 pM, cluster amplified on a single lane of v3 flowcell and sequenced with 2×101 bp paired end reads and a 7 bp index read using SBS v3 chemistry on a HiSeq2000 (Illumina, San Diego, CA). Samples were also subjected to the Foundation Medicine T5a test, a cancer genome profiling test based on massively parallel DNA sequencing that also uses capture based targeted sequencing (Frampton et al., 2013), substantially overlaps the BROCA test and includes many additional genes that are considered actionable in different tumor types.

2.7. Mutation analysis

The BROCA panel identifies all classes of mutations, including single-base substitutions, small insertions and deletions, and large gene rearrangements (Walsh et al., 2011). Sequence alignment and variant calling were performed against the reference human genome (UCSC hg19) as previously described (Walsh et al., 2011). Each variant was annotated with respect to gene location and predicted function in HGVS nomenclature. Deletions and duplications of exons were detected by a combination of depth of coverage and split read analysis. Missense variants without clear deleterious impact were not routinely included. For somatic large gene rearrangements or copy number variations (CNVs), any intragenic deletion or duplication was considered deleterious. Homozygous whole gene deletions were considered deleterious; hemizygous whole gene deletions (i.e., loss of heterozygosity (LOH)) were excluded. All sequence variants were confirmed with Sanger sequencing. Germline analysis of BRCA1/2 mutations identified in baseline HG-SOC was performed in germline DNA with Sanger Sequencing in two independent laboratories (SF and EMS), yielding concordant results. Due to the need to maintain patient deidentification in this consecutive, single institution series, individual germline results have not been reported.

2.8. BRCA1 methylation analysis

Five hundred ng of neoplastic DNA was bisulfite converted with an EZ Methylation Direct kit (Zymo Research, Irvine, CA) and evaluated with methylation sensitive PCR as previously described (Esteller et al., 2000). In vitro methylated DNA (ZymoResearch, CA) was used as a positive control.

2.9. Western blotting

Whole PDX tumor lysates were generated by grinding tumor fragments in a mortar and pestle with liquid nitrogen, then homogenizing with a poltyron and the addition of RIPA buffer (Sigma) and Protease inhibitor (Roche). Protein samples were probed with antibodies against Cyclin E (Clone HE12; Santa Cruz) and β-actin (clone AC-74, Sigma; also used as a loading control).

2.10. Statistical analysis

Prism (Version 5; GraphPad) and Excel (Version 12.2.8) software were used for statistical analysis. Mean and standard deviations were calculated using Excel. Two group comparisons were made using 2-tailed t tests assuming equal variances. The time taken for a PDX to develop to the pre-defined tumor volume at which euthanasia of the animal was required, was calculated and plotted using Kaplan−Meier curves (Prism version 5). Differences in time taken to volume required for cull post treatment, between cohorts of treatment mice, were tested using log-rank tests. P values less than 0.05 were considered to indicate statistical significance.

3. Results

3.1. HG-SOC cohort and BRCA1/BRCA2 status

Potentially high-grade OC samples were collected based on frozen section diagnosis at the time of primary cytoreductive surgery and transplanted into NOD/SCID IL2Rγ^{null} recipient mice. Twelve samples transplanted were confirmed to be viable HG-SOC following histopathologic review. This cohort of HG-SOC patients was representative of those described in larger clinical series (Supplementary Table 1). Four patients had significant family histories of breast cancer or OC and none were known to carry germline mutations in BRCA1 or BRCA2 at the time of diagnosis. Five women were less than 60 years old, including two of the four women with a positive family history (Supplementary Table 1).

IHC confirmed positive expression for WT1 and PAX8 as well as variable expression for the estrogen receptor, progesterone receptor and proliferative marker Ki67 (strong staining, $n = 10$; moderate staining, $n = 2$) (Supplementary Figures S1−S3). As expected (Ahmed et al., 2010), staining for p53 protein was strong in nine cases, consistent with a mutation in TP53, and absent in three, consistent with loss of the transcript due to mutation (Supplementary Table S2 and Supplementary Figures S1, S3A). Sequencing of DNA repair genes involved in the FA-BRCA-HR pathway (Supplementary Table S3) confirmed that all 12 HG-SOC contained mutations

Table 1 − Molecular Characteristics of HG-SOC transplanted.

HG-SOC	Mutation[a]	MYCN[c]	LIN28B[c]	CCNE1[c]	CCNE1[d]	BCL-2[d]	BCL-x$_L$[d]
5	BRCA2	+	++	+	+	++	+
11	nmf[b]	++	+	+	+	+	+
13	BRCA2	+	−	−/+	+	+	+
19	BRCA2	−/+	−	+	+	+	+
20[f]	nmf	+++	++	+	nd	nd	nd
27	nmf	+	+	+	+	++	+
28[f]	PMS2	+	++	+	nd	nd	nd
29	nmf	+++	+++	+++	+++	+++	+
36	nmf	+	+++	+	nd	+++	+
54	BRCA1	+	+	++	+	+	+
56	BRCA1	+	+	+	+	+	+
62	nmf	+	++	+++	+++[e]	+	+

Analysis of baseline HG-SOC: DNA repair genes by BROCA sequencing (by Walsh et al., 2011); qRT-PCR and IHC. Six HG-SOC were found to harbor a mutation in a DNA repair gene, other than TP53. Three HG-SOC were found to contain the highest levels of oncogene over-expression by qRT-PCR (see Supplementary Figure S8) or IHC (see Figure 4 and Supplementary Figure S9).
nd = not done due to lack of sample material. −/+ negligible expression, + low expression, ++ intermediate expression, +++ high expression relative to this cohort and control cell lines. Positive control cell lines: OVCAR3, known to be amplified for CCNE1; CH1, known to have over-expression of MYCN. qRT-PCR average of 3−7 experiments (one baseline RNA sample per HG-SOC). IHC, scored by two independent investigators, minimum 200 consecutive tumor nuclei.
a BROCA sequencing (Walsh et al., 2011).
b nmf − no mutation found in DNA repair genes (apart from in TP53) (see Supplementary Table S2).
c qRT-PCR.
d IHC.
e Heterogenous expression for#62.
f Failed to transplant (no PDX generated).

in TP53 (Supplementary Table S2). Two HG-SOC were found to contain mutations in BRCA1, three HG-SOC had mutations in BRCA2 and a sixth had a mutation in PMS2, a Lynch syndrome family gene associated with OC (de la Chapelle, 2004) (Tables 1 and 2, Supplementary Tables S1, S4). Five of six patients with HG-SOC bearing a DNA repair gene mutation were either <60 years old, had a positive family history or both (Supplementary Table S1). Four of the five deleterious mutations in BRCA1/2 were frameshift mutations and one was a missense mutation previously reported as pathogenic

Table 2 − In vivo cisplatin response of PDX compared with clinical outcome.

PDX in vivo cisplatin response		BRCA1 or BRCA2 mutation			No mutation found	
Sensitive ≥100 d		#5 [BRCA2]	#19 [BRCA2]	#56 [BRCA1]	#11 [BRCA1 methylated]	
	1st TFI	10	17[c]	>7	>21	
	Alive[a]	30	23	12	25	
Resistant <100 d		#13 [BRCA2]	#54 [BRCA1]		#27	
	1st TFI	5	>9		17[b]	
	Alive[a]	No, 14	13		22	
Resistant/Refractory					#62 [BRCA1 methylated] CCNE1hi[d]	
	1st TFI				>6	
	Alive[a]				10	
Refractory					#29 CCNE1/MYCN/LIN28B/BCL2hi	#36 LIN28B/BCL2 hi
	1st TFI				NA	3
	Alive[a]				No, <1	16

Patient-Derived Xenograft (PDX) classified by in vivo cisplatin response (maximal sensitivity to least sensitivity indicated by the arrow) and presence or absence of DNA repair gene mutations (Walsh et al., 2011) (apart from in TP53). No mutation found by BROCA sequencing (Walsh et al., 2011) of DNA repair genes. Clinical course for the patient from whom the PDX was derived: all patients received a first treatment regimen consisting of 6 cycles of platinum-based chemotherapy, apart from Patient #29 who was too unwell for treatment. Patient #5 had dose delays and dose reductions due to toxicity. TFI − Treatment Free Interval in months = date of last dose of prior regimen of systemic chemotherapy until date of first dose of next regimen systemic chemotherapy.
[BRCA1/2] = BRCA1/2 mutation.
a Survival in months post date of initial surgical resection.
b Clinical trial involving standard chemotherapy with placebo/novel agent, followed by maintenance therapy with placebo/novel agent.
c No reversion of BRCA2 mutation in patient sample of recurrent tumor.
d CCNE1 expression in baseline HG-SOC was heterogenous (Supplementary Figure S9A).
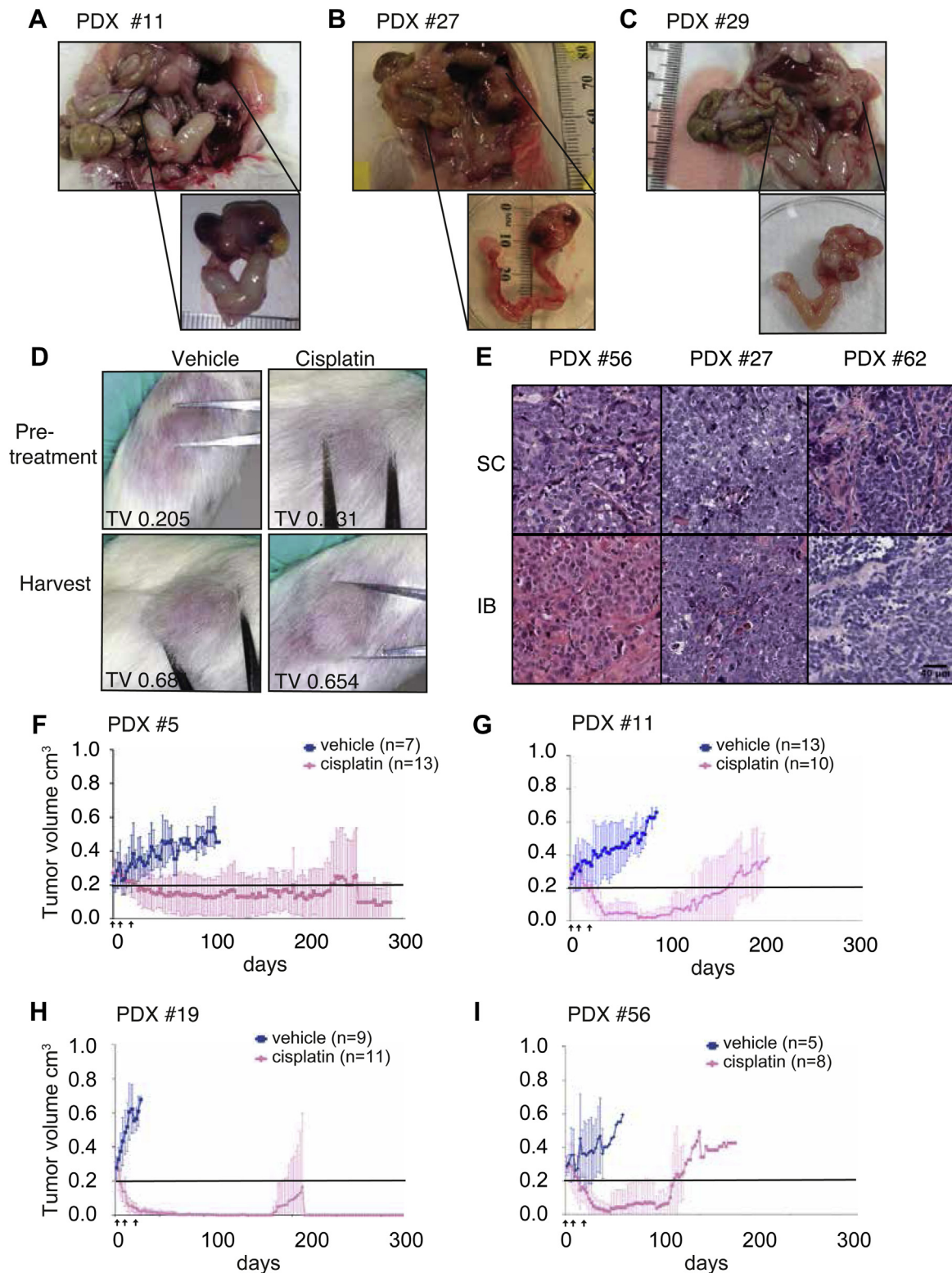
Figure 1 – Generation of HG-SOC patient-derived xenografts. (A–C) Photographs of intra-bursal (IB) patient-derived xenografts (PDX) upon harvest. (D) Photographs of subcutaneous (SC) PDX prior to administration of vehicle or cisplatin; and prior to harvest upon progressive disease, following either vehicle or cisplatin. (E) H + E images of PDX tumor morphology following xenotransplantation in either the SC or IB sites. (F–H) Mean tumor volume (cm^3) following treatment with cisplatin. PDX #5, #11, #19 and #56 were sensitive to treatment with cisplatin. Recipient mice bearing Transplantation T2-3 PDX were randomized to treatment with vehicle or cisplatin 4 mg/kg, D1, 8, 18. Tumor measurements were monitored up to three times per week. PDX were harvested at a tumor volume of 0.5–0.7 cm^3 or mice were re-treated with the same regimen at 0.5 cm^3. F, PDX #5 ^{BRCA2} T3, G, #11 T2, H, #19 ^{BRCA2} T3 and i, #56 ^{BRCA1} T2 demonstrated prolonged response to a single regimen of cisplatin (> 100 d) (see Supplementary Table 6 for median time to harvest and p values for difference). Discontinuity in graphs due to progressive disease in one recipient mice, whilst remaining mice had minimal tumor detected at that time. Error bars represent Standard Deviation (SD), n = individual mice.
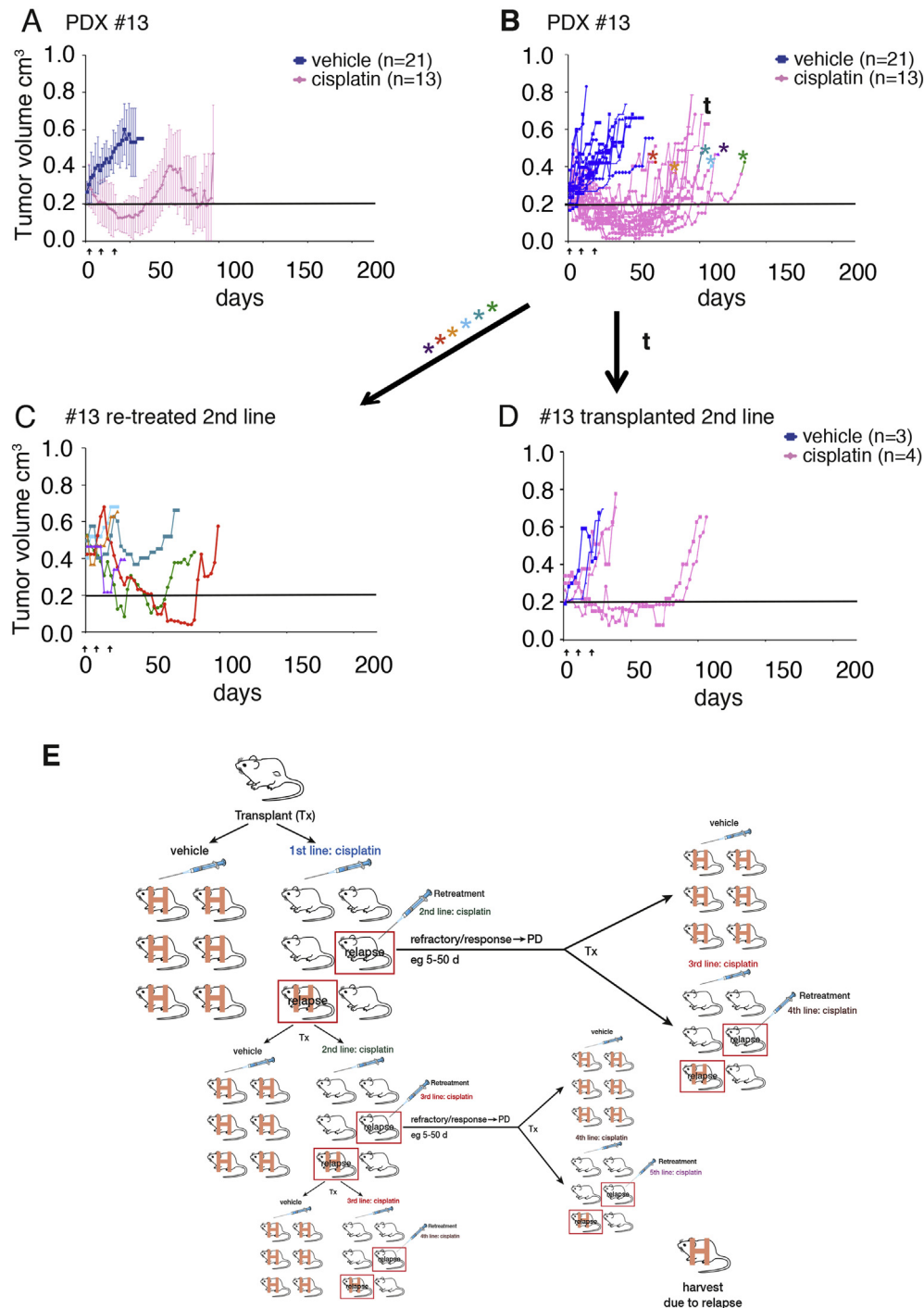
Figure 2 − Platinum-resistant HG-SOC patient-derived xenografts. PDX #13 was resistant to treatment with cisplatin. (A) Mean tumor volume (cm³) and B, responses for individual mice, following treatment with cisplatin. Recipient mice bearing T2 PDX were randomized to treatment with vehicle or cisplatin 4 mg/kg, D1, 8, 18. Tumor measurements were monitored up to three times per week. PDX were harvested at a tumor volume of 0.7 cm³ or re-treated with the same regimen at 0.5 cm³. During *in vivo* treatment with three doses of cisplatin, PDX #13 ^{BRCA2} T2 underwent initial tumor regression, however, this was followed by PD (defined as 20% increase in tumor volume compared with nadir) at 76 d (see Supplementary Table 6 for median time to harvest and *p* values for difference). Mice bearing recurrent tumours were randomly allocated either to (C) re-treatment with the same cisplatin regimen as before, when the tumor volume reached 0.5 cm³ ("re-treated 2nd-line") or (D) tumor was harvested at 0.7 cm³, transplanted and recipient mice were treated with vehicle or cisplatin ("transplanted 2nd-line"). Coloured asterixes in (B) correspond to coloured lines in (C). Error bars represent Standard Deviation (SD), *n* = individual mice. (E) Model of driving platinum resistance: Recipient mice bearing T2 or T3 PDX were randomized to treatment with vehicle or cisplatin 4 mg/kg, D1, 8, 18. Recipient mice with refractory or progressive disease were re-treated at a tumor volume of 0.5 cm³ with the same cisplatin regimen as before, in order to determine cisplatin sensitivity ("re-treated 2nd-line cisplatin"). Some recipient mice had cisplatin-refractory disease following first-line therapy. Randomly selected
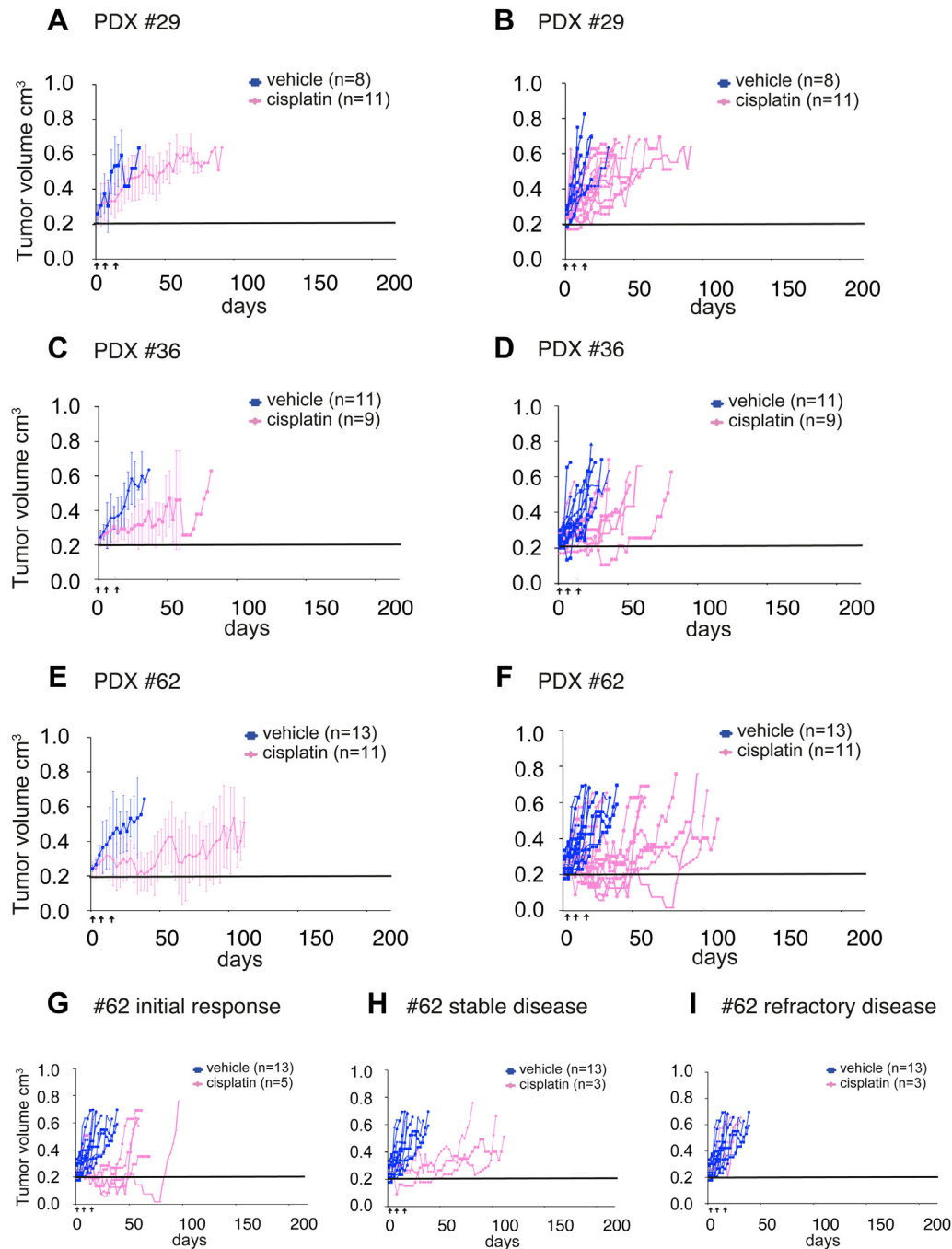
Figure 3 − Platinum-refractory HG-SOC patient-derived xenografts. PDX #29, #36 and #62 resulted in refractory responses to treatment with cisplatin. Recipient mice bearing T2-3 PDX were randomized to treatment with vehicle or cisplatin 4 mg/kg, D1, 8, 18. Tumor measurements were monitored up to three times per week. PDX were harvested at a tumor volume of 0.7 cm³ (A, C, E) Mean tumor volume (cm³) following treatment with cisplatin. (B, D, F) Responses for individual mice. All PDX #29 T2 recipients had cisplatin-refractory disease requiring euthanasia during cisplatin therapy, such that no mice were available for re-treatment. For PDX #36 T3, a subset of mice had (G) initial response (PR) followed by PD (median survival cisplatin 56 d vs vehicle 17 d $p = 0.0004$); (H) a subset of mice had stable disease followed by PD (median survival cisplatin undefined vs vehicle 17 d $p = 0.0044$); and (I) a subset of mice had refractory disease whilst on cisplatin (median survival cisplatin 27 d vs vehicle 17 d $p = 0.819$) (see Supplementary Table 6 for median time to harvest and p values for difference). Error bars represent Standard Deviation (SD), $n =$ individual mice.

recurrent PDX were harvested for analysis and were serially transplanted at tumor volume of 0.5−0.7 cm³ for treatment (transplanted 2nd-line cisplatin). This iterative process of "driving platinum resistance" was then repeated, with 3rd-line treatments, generating increasingly platinum-resistant/refractory samples. H indicates Harvest.

(Easton et al., 2007). For the five BRCA1 or BRCA2 mutations documented in baseline tumor DNA, two were also documented in the germline (one each in BRCA1 and BRCA2) and the remaining three mutations were found to be somatic (not detected in the germline by Sanger sequencing). Methylation analysis of BRCA1 determined that HG-SOC #11 and #62 contained methylated BRCA1 (Supplementary Figure S4).

3.2. Generation of HG-SOC PDX with stable cisplatin-response phenotype

In order to generate PDXs, we combined the following approaches: use of unmanipulated tumor fragments (to prevent in vitro artifact); both orthotopic intra-ovarian bursal (IB) and the subcutaneous (SC) routes (Figure 1A–E); the use of NOD/SCID IL2Rγ^{null} recipient mice, which have been shown to result in higher xenotransplantation rates (Quintana et al., 2008); concomitant administration of estradiol pellets in the contralateral flank for SC transplants; and molecular and functional annotation to increase the therapeutic utility of the PDX panel. Of 12 HG-SOC transplanted and followed for 300 days, ten HG-SOC xenografted successfully (success rate of 83%), including all five BRCA1/2-defective HG-SOCs (100%) and five out of seven (71%) with no FA-BRCA-HR pathway mutations (HR WT) (Supplementary Table S5). All T1 (first transplantation) PDXs were confirmed as being of epithelial origin (pan-CK positive) (Supplementary Figure S3B). Both the IB and SC routes resulted in reliable transplantation and histologic appearance of H + E stained sections of SC versus IB (orthotopic) PDXs was similar, with serous papillary structures present in PDXs from both sites (Figure 1E). As the SC route is less invasive and allows more accurate measurement of tumor volume, we chose that route for the majority of analyses beyond T2. Expression of WT1, PAX8, ER, PR, p53 and Ki67 in serial HG-SOC PDXs was largely consistent with baseline patterns (Supplementary Figure S1–S2). The PDX in which we observed the most change in morphology was #29 (Supplementary Figure S1–S2), which also proved to be the most refractory to treatment.

Because of the important prognostic information provided by the clinical response to platinum-based chemotherapy (Bookman et al., 2009), we determined the in vivo response to cisplatin for each PDX, using single agent cisplatin, representing platinum-based therapy in women. We defined response as being "cisplatin sensitive" if the average PDX tumor volume of the recipient mice underwent initial tumor regression with complete remission (CR, defined as tumor volume < 0.2 cm^3) or partial remission (PR, defined as reduction in tumor volume of >30% from baseline) followed by progressive disease (PD, an increase in tumor volume of >20% from 0.2 cm^3 or nadir post-treatment, if nadir ≥0.2 cm^3) occurring ≥100 days from start of treatment; "cisplatin resistant" if initial tumor regression (CR or PR) or stable disease (SD) was followed by PD within 100 days; or "cisplatin refractory" if three or more mice bearing that PDX had tumors which failed to respond (no CR, PR or SD) during cisplatin treatment (day 1–18). Four PDX (PDX #5, #11, #19 and #56) were sensitive to cisplatin, three PDX were resistant (PDX #13, #27 and #54) and three PDX were refractory (PDX #29, #36 and #62) (Figures 1–3, Supplementary Figure S5, S6). Similar cisplatin response was observed after serial passage of PDXs without intervening treatment (transplantation

T2–4), suggesting that cisplatin response was a stable phenotype using the fragment (undigested) approach (Supplementary Figure S6). The relative growth rates for each PDX are indicated by the median survival of the vehicle-treated mice (Supplementary Table S6).

3.3. Cisplatin-sensitive PDX with BRCA1/2 mutations

During in vivo treatment with cisplatin, PDXs #5, #11, #19 and #56 were "cisplatin sensitive," with PD at >280 days for #5, day 247 for #19, day 171 for #11 and day 120 for #56 (Table 2, Supplementary Table S6 and Figure 1). Three of these four cisplatin-sensitive PDXs harbored BRCA1 or BRCA2 mutations. In comparison, PDX #13, #27 and #54 were "cisplatin resistant," with initial tumor regression, followed by PD at 76, 62 and 54 days respectively; and PDX #29, 36 and 62 were platinum refractory, with PD occurring during treatment on days 6, 22 and 43, respectively (Table 2, Supplementary Table S6, Figure 3, Supplementary Figures S5–S7). For PDX #36 and #62, in addition to generating recipient mice displaying a cisplatin-refractory response, a subset of mice had "cisplatin resistant" disease, i.e., either initial regression or stable disease followed by PD within 100 days (Figure 3, Supplementary Figure S6). Of the three cisplatin resistant PDXs, two were mutant for BRCA1/2 (Table 2). As poor response to platinum therapy in BRCA1/2 mutation carriers can be seen in the clinic (Table 2 and (TCGA (2011))), these PDXs will be valuable for further study of this phenotype. Of the three cisplatin-refractory PDXs, none were mutant for BRCA1/2 (Table 2).

In order to determine second-line platinum response, mice bearing recurrent tumors were randomly allocated either to re-treatment with the same cisplatin regimen as before when the tumor volume reached 0.5 cm^3 ("re-treated 2nd-line", Figure 2C and Supplementary Figure S5C) or tumor was harvested at 0.7 cm^3, transplanted and recipient mice were treated with vehicle or cisplatin ("transplanted 2nd-line", Figure 2D and Supplementary Figure S5D). Re-treatment of a mouse with second-line cisplatin resulted in similar or shorter time in days from final dose of treatment to tumor volume of 0.5 cm^3, compared to first-line treatment of that same mouse (from final dose of first-line treatment to first date of re-treatment or Treatment Free Interval) (Supplementary Table S7). At the time of re-treatment with second-line cisplatin, the tumor volume was larger than at time of first-line treatment, as is usually the case in the clinic (as most patients undergo primary but not secondary debulking surgery prior to platinum-based chemotherapy). Some "re-treated 2nd-line cisplatin" mice developed cisplatin-refractory disease and these samples were noted for further studies. This iterative process of "driving platinum resistance" (Figure 2E) was then repeated, with 3rd-line treatments, generating increasingly platinum-resistant/refractory serial samples, as occurs in the clinical setting following subsequent rounds of platinum-based chemotherapy.

3.4. Cisplatin-refractory PDXs derive from HG-SOC with over-expression of oncogenes

In order to explore causes of primary drug resistance, we screened for over-expression of oncogenes, including CCNE1

(Etemadmoghadam et al., 2010), the MYCN pathway (Helland et al., 2011) and the BCL2 family (Cragg et al., 2009). Analysis by qRT-PCR detected increased expression of CCNE1 and/or MYCN or LIN28B (a member of the MYCN pathway) mRNA in HG-SOC #29, #36 and #62 (Table 1 and Supplementary Figure S8). Homogenous levels of expression of mRNA for HMGA2 (MYCN pathway) were observed (data not shown). IHC for Cyclin E confirmed highest expression in HG-SOC #29 and heterogenous expression in #62 (Tables 1 and 2, Figure 4 and Supplementary Figure S9B–C), which was confirmed by western blotting (Supplementary Figure S9D). Consistent with the heterogenous expression by IHC, differing levels of CCNE1 mRNA were observed by qRT-PCR in tumours from mice bearing various aliquots of PDX #62. Individual mice bearing PDX #62 aliquots with the shortest response time to cisplatin had the highest level of CCNE1 expression (Supplementary Figure S9, r-squared value 0.6163, slope (95% CI) −31.29 (−53.35 to −9.222)). Bcl-2 protein expression was highest in HG-SOC #29 and 36 (Bcl-x_L was low in all) (Tables 1 and 2, Figure 4 and Supplementary Figure S9A). In other words, the three PDXs that were refractory to cisplatin were derived from the three HG-SOCs with overexpression of one or more oncogenes at baseline (no DNA repair gene mutations were detected in tumors giving rise to these three PDXs).

In order to provide a less directed molecular analysis of the ten PDXs studied here, genomic profiling of PDX DNA (fresh PDX tumor) was performed using the Foundation Medicine next generation sequencing (NGS) platform (T5a Test), which interrogates 287 genes as well as 47 introns of 19 genes involved in rearrangements. The deleterious mutations in TP53 and either BRCA1 or BRCA2 were all confirmed (Supplementary Table S8). As expected for HG-SOC (TCGA, 2011) a paucity of additional mutations (likely to be somatic) were observed. Those mutations detected (only 1–2 mutations per PDX) were found in PDX containing mutations in either BRCA1 or BRCA2 or methylation of BRCA1. In contrast, all three refractory PDX were noted to have multiple other types of genetic aberrations, including oncogenic amplifications (CCNE1 amplification confirmed in PDX #29; amplification of MCL1, an antiapoptotic BCL2 paralog, also noted).

3.5.   PDX cisplatin response consistent with clinical outcome

PDX cisplatin response and matched patient data were compared (Table 2). All four cisplatin-sensitive PDXs derived from patients who had platinum-sensitive HG-SOC, remaining in remission for more than six months following cessation of first-line platinum-based chemotherapy (first treatment-free interval (TFI) 10, >21, 17 and >7 months respectively; overall survival (OS) to date (all alive) 30, 25, 23 and 12 months, respectively) (Table 2). In contrast, the six PDXs designated as cisplatin-resistant or -refractory derived from patients who tended to experience a worse outcome (Table 2). The three patients whose HG-SOCs overexpressed oncogenes and generated cisplatin-refractory PDXs had the poorest outcomes: the most refractory PDX, #29, derived from a patient who was too unwell to be treated and died <1 month post diagnosis; the second refractory PDX, #36, derived from a patient who had a short first TFI of just three months, followed by a second

TFI of < one month. Accordingly, even though single-agent cisplatin is not identical to regimens used in the clinic (and is not preceded by debulking surgery), the PDX "platinum response" appears to broadly reflect patient outcome, identifying platinum-sensitive, resistant and refractory groups of HG-SOC PDX for further study.

4.   Discussion

For women with HG-SOC, there is an urgent need to develop precision therapies targeted to the drivers and susceptibilities of their cancers. There have been several barriers to the development of these treatments. First, it is difficult to obtain OC samples pre- and post-drug treatment in the clinic, making it hard to determine whether the intended target has been inhibited in the clinical setting. In addition, the five most commonly published ovarian cancer cell lines, usually studied to reflect HG-SOC, do not in fact closely resemble HG-SOC (Domcke et al., 2013), further emphasizing the urgent need for new HG-SOC models. In this context, we have developed a murine PDX approach based on consecutive chemotherapy-naïve HG-SOCs, with a high transplantation success rate (83%) and stability of cisplatin-response phenotype. Cisplatin response in this PDX model is reflective of the clinical outcome of the corresponding patient. These new models enable future sophisticated pre-clinical analysis, including clonal analysis based on driving platinum resistance, to determine the therapeutic potential of novel agents targeted to individual HG-SOC PDX. PDX models such as these will, therefore, enhance future understanding of response to current therapies as well as design of precision therapies for women with HG-SOC.

Although a number of studies have previously reported the derivation of HG-SOC PDXs, the responses to conventional or targeted therapeutics have only been described in association with molecular annotation for 1–2 independent HG-SOC PDX models per report (Faratian et al., 2011; Kortmann et al., 2011; Press et al., 2008; Sims et al., 2012). Moreover, previous reports provide little information about patient outcome. Here we have attempted to characterize a group of HG-SOC PDXs in detail in order to assess the factors that determine response to platinum therapy, the most widely used and most effective treatment currently available for this disease (Bookman et al., 2009).

At present the most important prognostic indicator of clinical outcome following the conclusion of surgical management is the response of the HG-SOC to platinum-based therapy (Vaughan et al., 2011). HG-SOCs with germline or somatic BRCA1 or BRCA2 mutations are associated with improved survival compared to HG-SOCs known to not have BRCA1 or BRCA2 mutations (Alsop et al., 2012; Kaye et al., 2012; TCGA, 2011). Accordingly, we characterized individual HG-SOCs and resultant PDXs according to in vivo platinum response and DNA repair gene status, including BRCA1 and BRCA2 and other genes in the FA-BRCA-HR pathway. Of the first ten PDXs generated, five harbored a mutation in either BRCA1 or BRCA2. This is in marked contrast to established human ovarian cancer cell lines, which contain BRCA1 and BRCA2 mutations only rarely (Domcke et al., 2013; Stordal et al., 2013). Three of four platinum sensitive HG-SOC PDXs contained DNA repair gene mutations,
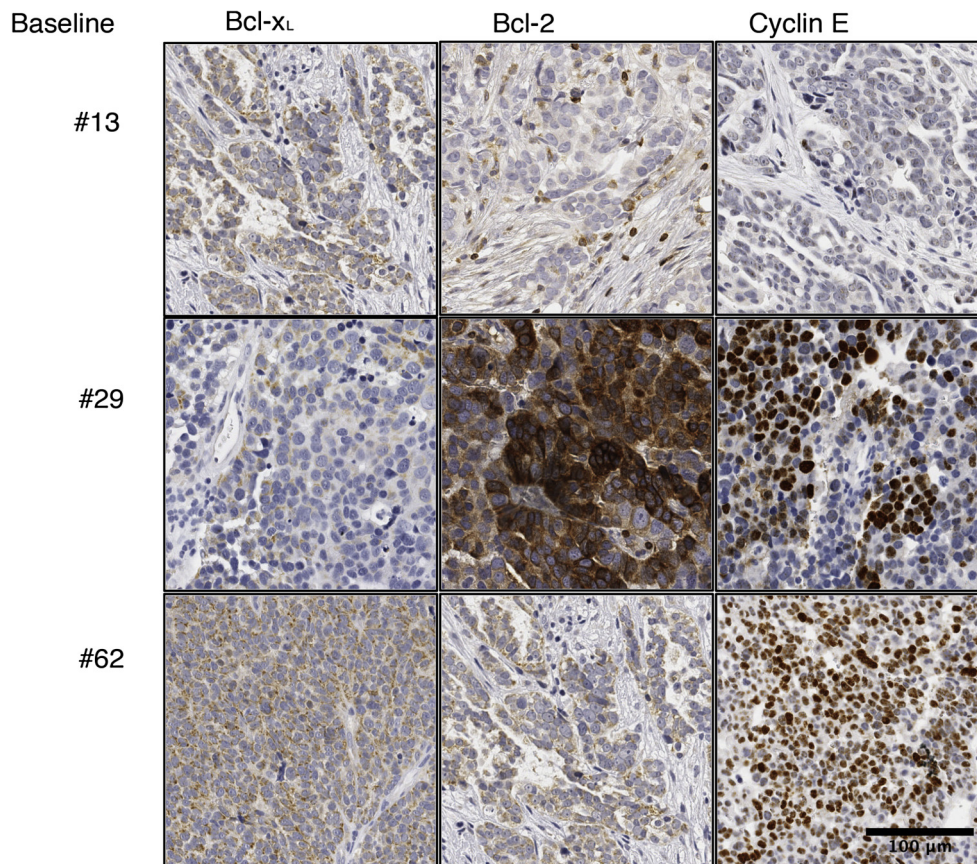
Figure 4 — Oncogene overexpression in HG-SOC. IHC analysis of Bcl-xL, Bcl-2 and Cyclin E for baseline HG-SOC. HG-SOC #13 (low staining for Bcl-xL, Bcl-2 and Cyclin E), #29 (strong staining for Bcl-2 and Cyclin E) and #62 (heterogenous staining for Cyclin E: some areas with strong staining, some with less). HG-SOC #29 and #36 gave rise to cisplatin-refractory PDX (some images repeated in Supplementary Figure S9).

as did two of six platinum-resistant or -refractory PDX. Accordingly, it appears that defects in HR are necessary but not sufficient for platinum sensitivity.

In order to drive cisplatin-resistance, we re-challenged recurrent PDXs with sequential second- and third-line platinum regimens, as occurs in the clinic. For cisplatin-resistant PDXs, we generated serial PDX samples some of which, under the pressure of subsequent platinum-based treatment, became increasingly resistant (initial sensitivity followed by more rapid relapse) or refractory to cisplatin, compared with the initial round of therapy, thus supporting the clinical relevance of our model.

A subset of the ten PDXs may represent women diagnosed with HG-SOCs that are poorly responsive, or in some cases unresponsive, to primary platinum-based therapy, with a very high short-term mortality. Three of ten PDXs gave rise to primary cisplatin-refractory disease; and all were derived from HG-SOCs that overexpressed dominant oncogenes (*CCNE1*, *LIN28B* and/or *BCL-2*) known to be associated with poor prognosis in HG-SOC (Etemadmoghadam et al., 2010; Helland et al., 2011) or other tumor types (Cragg et al., 2009). In contrast, none of the cisplatin-sensitive PDXs overexpressed these genes. Foundation Medicine testing was broadly consistent, with the majority of oncogenic amplifications occurring in cisplatin-refractory

PDXs. Indeed, this PDX model highlights as "cisplatin-refractory" those HG-SOCs with the poorest prognosis. Thus, this PDX model may be particularly useful for further exploring the causes and treatment of platinum resistant disease in the clinic.

Whilst PDX do not allow the study of pre-cancerous stages which led to the development of the HG-SOC, nor is manipulation of the immune system possible in an immune-deficient mouse, there are many advantages. The use of viable freezings of minced tumor provide a renewable resource which enables response to multiple drugs to be determined and resistance to be analysed in responders vs non-responders in sequential tumor biopsies. This enables study of how an HG-SOC might evolve under pressure of a certain drug, that is more comprehensive than can be obtained in clinical specimens. Detailed studies of stroma could be attempted by studying the replacement of human stroma by mouse stroma, and the levels of candidate genes or proteins in the stroma associated with HG-SOC from differing molecular sub-types. The present HG-SOC PDX cohort will also allow us to specifically target novel therapeutic approaches *in vivo*, such as PARP inhibitors for DNA repair defective HG-SOC, to better understand the implications for patients. By allowing the generation of serial samples, the PDX models will also facilitate the study of therapy-driven clonal evolution.

5.   Conclusion

This consecutive cohort of HG-SOC PDX reflect clinical platinum response. Three of four platinum-sensitive PDXs contained mutations in the DNA repair genes, BRCA1 or BRCA2 and, in contrast, overexpression of oncogenes was observed in all three platinum refractory PDXs. Using this PDX system to define platinum-response, DNA repair gene and oncogene status, PDXs can be stratified for treatment with novel therapies, such as PARP inhibitor therapy or therapies targeting specific oncogenes. It is not practical to generate such labor intensive and expensive analyses for the majority of patients. Instead, insights from this PDX model may improve design of future clinical trials of novel targeted agents, leading to much needed improvements in therapeutic options for women with OC.

Author contributions

MT planned experiments, interpreted data and wrote the manuscript. LH, MC, LM, EB, JP, MH, SA, VH, DE, KA, LG, SF, JBK and EMS helped with experimental design, contributed data. OM contributed samples and helped with interpretation of results. JP, KA, GM, KH, SHK, EMS and DDB helped with interpretation of results and manuscript writing. CLS and MW conceived of the study, planned experiments, interpreted data and wrote the manuscript. All authors reviewed the manuscript.

Acknowledgments

Appendix A.
Supplementary data

Supplementary data related to this article can be found at http://dx.doi.org/10.1016/j.molonc.2014.01.008.

R E F E R E N C E S

Ahmed, A.A., Etemadmoghadam, D., Temple, J., Lynch, A.G., Riad, M., Sharma, R., Stewart, C., Fereday, S., Caldas, C., Defazio, A., et al., 2010. Driver mutations in TP53 are ubiquitous in high grade serous carcinoma of the ovary. J. Pathol. 221, 49–56.

Alsop, K., Fereday, S., Meldrum, C., Defazio, A., Emmanuel, C., George, J., Dobrovic, A., Birrer, M.J., Webb, P.M., Stewart, C., et al., 2012. BRCA mutation frequency and patterns of treatment response in BRCA mutation-positive women with ovarian cancer: a report from the Australian Ovarian Cancer Study Group. J. Clin. Oncol. 30 (21), 2654–63.

Audeh, M.W., Carmichael, J., Penson, R.T., Friedlander, M., Powell, B., Bell-McGuinn, K.M., Scott, C., Weitzel, J.N., Oaknin, A., Loman, N., et al., 2010. Oral poly(ADP-ribose) polymerase inhibitor olaparib in patients with BRCA1 or BRCA2 mutations and recurrent ovarian cancer: a proof-of-concept trial. Lancet 376, 245–251.

Barber, L.J., Sandhu, S., Chen, L., Campbell, J., Kozarewa, I., Fenwick, K., Assiotis, I., Rodrigues, D.N., Reis Filho, J.S., Moreno, V., et al., 2013. Secondary mutations in BRCA2 associated with clinical resistance to a PARP inhibitor. J. Pathol. 229, 422–429.

Beroukhim, R., Mermel, C.H., Porter, D., Wei, G., Raychaudhuri, S., Donovan, J., Barretina, J., Boehm, J.S., Dobson, J., Urashima, M., et al., 2010. The landscape of somatic copy-number alteration across human cancers. Nature 463, 899–905.

Bookman, M.A., 2011. Update of randomized trials in first-line treatment. Ann. Oncol. Off. J. Eur. Soc. Med. Oncol./ESMO 22 (Suppl. 8), viii52–viii60.

Bookman, M.A., Brady, M.F., McGuire, W.P., Harper, P.G., Alberts, D.S., Friedlander, M., Colombo, N., Fowler, J.M., Argenta, P.A., De Geest, K., et al., 2009. Evaluation of new platinum-based treatment regimens in advanced-stage ovarian cancer: a Phase III Trial of the Gynecologic Cancer Intergroup. J. Clin. Oncol. Off. J. Am. Soc. Clin. Oncol. 27, 1419–1425.

Cragg, M.S., Harris, C., Strasser, A., Scott, C.L., 2009. Unleashing the power of inhibitors of oncogenic kinases through BH3 mimetics. Nat. Rev. Cancer 9, 321–326.

de la Chapelle, A., 2004. Genetic predisposition to colorectal cancer. Nat. Rev. Cancer 4, 769–780.

Domcke, S., Sinha, R., Levine, D.A., Sander, C., Schultz, N., 2013. Evaluating cell lines as tumour models by comparison of genomic profiles. Nat. Commun. 4, 2126.

Easton, D.F., Deffenbaugh, A.M., Pruss, D., Frye, C., Wenstrup, R.J., Allen-Brady, K., Tavtigian, S.V., Monteiro, A.N., Iversen, E.S., Couch, F.J., et al., 2007. A systematic genetic assessment of 1,433 sequence variants of unknown clinical significance in the BRCA1 and BRCA2 breast cancer-predisposition genes. Am. J. Hum. Genet. 81, 873–883.

Edwards, S.L., Brough, R., Lord, C.J., Natrajan, R., Vatcheva, R., Levine, D.A., Boyd, J., Reis-Filho, J.S., Ashworth, A., 2008. Resistance to therapy caused by intragenic deletion in BRCA2. Nature 451, 1111–1115.

Esteller, M., Silva, J.M., Dominguez, G., Bonilla, F., Matias-Guiu, X., Lerma, E., Bussaglia, E., Prat, J., Harkes, I.C., Repasky, E.A., et al., 2000. Promoter hypermethylation and BRCA1

inactivation in sporadic breast and ovarian tumors. J. Natl. Cancer Inst. 92, 564–569.

Etemadmoghadam, D., George, J., Cowin, P.A., Cullinane, C., Kansara, M., Gorringe, K.L., Smyth, G.K., Bowtell, D.D., 2010. Amplicon-dependent CCNE1 expression is critical for clonogenic survival after cisplatin treatment and is correlated with 20q11 gain in ovarian cancer. PloS One 5, e15498.

Faratian, D., Zweemer, A.J., Nagumo, Y., Sims, A.H., Muir, M., Dodds, M., Mullen, P., Um, I., Kay, C., Hasmann, M., et al., 2011. Trastuzumab and pertuzumab produce changes in morphology and estrogen receptor signaling in ovarian cancer xenografts revealing new treatment strategies. Clin. Cancer Res. An Off. J. Am. Assoc. Cancer Res. 17, 4451–4461.

Frampton, G.M., Fichtenholtz, A., Otto, G.A., Wang, K., Downing, S.R., He, J., Schnall-Levin, M., White, J., Sanford, E.M., An, P., et al., 2013. Development and validation of a clinical cancer genomic profiling test based on massively parallel DNA sequencing. Nat. Biotechnol. 31, 1023–1031.

Helland, A., Anglesio, M.S., George, J., Cowin, P.A., Johnstone, C.N., House, C.M., Sheppard, K.E., Etemadmoghadam, D., Melnyk, N., Rustgi, A.K., et al., 2011. Deregulation of MYCN, LIN28B and LET7 in a molecular subtype of aggressive high-grade serous ovarian cancers. PloS One 6, e18064.

Kaye, S.B., Lubinski, J., Matulonis, U., Ang, J.E., Gourley, C., Karlan, B.Y., Amnon, A., Bell-McGuinn, K.M., Chen, L.M., Friedlander, M., et al., 2012. Phase II, open-label, randomized, multicenter study comparing the efficacy and safety of olaparib, a poly (ADP-ribose) polymerase inhibitor, and pegylated liposomal doxorubicin in patients with BRCA1 or BRCA2 mutations and recurrent ovarian cancer. J. Clin. Oncol. Off. J. Am. Soc. Clin. Oncol. 30, 372–379.

Kortmann, U., McAlpine, J.N., Xue, H., Guan, J., Ha, G., Tully, S., Shafait, S., Lau, A., Cranston, A.N., O'Connor, M.J., et al., 2011. Tumor growth inhibition by olaparib in BRCA2 germline-mutated patient-derived ovarian cancer tissue xenografts. Clin. Cancer Res. Off. J. Am. Assoc. Cancer Res. 17, 783–791.

Ledermann, J., Harter, P., Gourley, C., Friedlander, M., Vergote, I., Rustin, G., Scott, C., Meier, W., Shapira-Frommer, R., Safra, T., et al., 2012. Olaparib maintenance therapy in platinum-sensitive relapsed ovarian cancer. N. Engl. J. Med. 366, 1382–1392.

Lee, C.H., Xue, H., Sutcliffe, M., Gout, P.W., Huntsman, D.G., Miller, D.M., Gilks, C.B., Wang, Y.Z., 2005. Establishment of subrenal capsule xenografts of primary human ovarian tumors in SCID mice: potential models. Gynecol. Oncol. 96, 48–55.

Narita, M., Nunez, S., Heard, E., Narita, M., Lin, A.W., Hearn, S.A., Spector, D.L., Hannon, G.J., Lowe, S.W., 2003. Rb-mediated heterochromatin formation and silencing of E2F target genes during cellular senescence. Cell 113, 703–716.

Norquist, B., Wurz, K.A., Pennil, C.C., Garcia, R., Gross, J., Sakai, W., Karlan, B.Y., Taniguchi, T., Swisher, E.M., 2011. Secondary somatic mutations restoring BRCA1/2 predict chemotherapy resistance in hereditary ovarian carcinomas. J. Clin. Oncol. Off. J. Am. Soc. Clin. Oncol. 29, 3008–3015.

Press, J.Z., Kenyon, J.A., Xue, H., Miller, M.A., De Luca, A., Miller, D.M., Huntsman, D.G., Gilks, C.B., McAlpine, J.N., Wang, Y.Z., 2008. Xenografts of primary human gynecological tumors grown under the renal capsule of NOD/SCID mice show genetic stability during serial transplantation and respond to cytotoxic chemotherapy. Gynecol. Oncol. 110, 256–264.

Quintana, E., Shackleton, M., Sabel, M.S., Fullen, D.R., Johnson, T.M., Morrison, S.J., 2008. Efficient tumour formation by single human melanoma cells. Nature 456, 593–598.

Roby, K.F., Taylor, C.C., Sweetwood, J.P., Cheng, Y., Pace, J.L., Tawfik, O., Persons, D.L., Smith, P.G., Terranova, P.F., 2000. Development of a syngeneic mouse model for events related to ovarian cancer. Carcinogenesis 21, 585–591.

Sakai, W., Swisher, E.M., Karlan, B.Y., Agarwal, M.K., Higgins, J., Friedman, C., Villegas, E., Jacquemont, C., Farrugia, D.J., Couch, F.J., et al., 2008. Secondary mutations as a mechanism of cisplatin resistance in BRCA2-mutated cancers. Nature 451, 1116–1120.

Sims, A.H., Zweemer, A.J., Nagumo, Y., Faratian, D., Muir, M., Dodds, M., Um, I., Kay, C., Hasmann, M., Harrison, D.J., et al., 2012. Defining the molecular response to trastuzumab, pertuzumab and combination therapy in ovarian cancer. Br. J. Cancer 106, 1779–1789.

Stewart, J.M., Shaw, P.A., Gedye, C., Bernardini, M.Q., Neel, B.G., Ailles, L.E., 2011. Phenotypic heterogeneity and instability of human ovarian tumor-initiating cells. Proc. Natl. Acad. Sci. U.S.A. 108, 6468–6473.

Stordal, B., Timms, K., Farrelly, A., Gallagher, D., Busschots, S., Renaud, M., Thery, J., Williams, D., Potter, J., Tran, T., et al., 2013. BRCA1/2 mutation analysis in 41 ovarian cell lines reveals only one functionally deleterious BRCA1 mutation. Mol. Oncol. 7, 567–579.

TCGA, 2011. Integrated genomic analyses of ovarian carcinoma. Nature 474, 609–615.

Vaughan, S., Coward, J.I., Bast Jr., R.C., Berchuck, A., Berek, J.S., Brenton, J.D., Coukos, G., Crum, C.C., Drapkin, R., Etemadmoghadam, D., et al., 2011. Rethinking ovarian cancer: recommendations for improving outcomes. Nat. Rev. Cancer 11, 719–725.

Walsh, T., Casadei, S., Lee, M.K., Pennil, C.C., Nord, A.S., Thornton, A.M., Roeb, W., Agnew, K.J., Stray, S.M., Wickramanayake, A., et al., 2011. Mutations in 12 genes for inherited ovarian, fallopian tube, and peritoneal carcinoma identified by massively parallel sequencing. Proc. Natl. Acad. Sci. U.S.A. 108 (44), 18032–7.